Use of power-averaging for quantifying the influence of structure organization on permeability upscaling in on-lattice networks under mean parallel flow

Jean-Raynald de Dreuzy, Paul de Boiry, Géraldine Pichot, Philippe Davy

Use of power averaging for quantifying the influence of structure organization on permeability upscaling in on-lattice networks under mean parallel flow

Jean-Raynald de Dreuzy,[1] Paul de Boiry,[1] Géraldine Pichot,[1] and Philippe Davy[1]

[1]   We numerically assess the relevance of power averaging as a means for permeability upscaling on a variety of 2D and 3D, dense, and sparse on-lattice networks. The power average exponent ω determined on a realization basis converges with the system size within the range of scales explored for all cases. Power averaging is strictly valid only for the 2D dense square case for which ω is equal to 0 with a numerical precision of 0.01 both for the lognormal and log-uniform permeability distributions consistently with the theoretical proof of Matheron (1967). For all other cases, the variability of ω with the local permeability distribution variance σ^2 is nonnegligible but remains small. It is equal to 0.09 for sparse networks and 0.14 for dense networks representing 4.5% and 7%, respectively, of the full possible range of ω values. Power averaging is not strictly valid but gives an estimate of upscaling at a few percent. Here ω depends slightly on the local permeability distribution shape beyond its variance but mostly on the morphological network structures. Most of the morphological control on upscaling for on-lattice structures is local and topological and can be explained by the dependence on the average number of neighbor by points (effective coordination number) within the flowing structure (backbone).

1.   Introduction

[2]   Upscaling permeability has been a very active research field for more than 20 years in hydrogeology [*Cushman*, 1986; *Cushman et al.*, 2002; *Neuman and Di Federico*, 2003; *Renard and Marsily*, 1997; *Sánchez-Vila et al.*, 1996, 2006; *Wen and Gómez-Hernández*, 1996]. Upscaling consists basically in deriving the equivalent permeability from the small-scale permeability distribution. Among the first results, the equivalent permeability of a 2D lognormally distributed permeability field has been found to be the geometric mean of the permeability distribution [*Matheron*, 1967]. For a layered medium, the equivalent permeability is equal either to the arithmetic mean for flow parallel to the layering or to the harmonic mean for flow perpendicular to the layering [*Cardwell and Parsons*, 1945]. In all these cases, upscaling consists in choosing the relevant average. More generally, *Desbarats* [1992a] proposed that the upscaling can be expressed as some power average of the permeability distribution. For a lognormal permeability distribution of geometric mean K_g and of lognormal standard deviation σ, the equivalent permeability K_{eq} is given by

$$K_{eq} = K_g \cdot \exp\left(\omega \cdot \frac{\sigma^2}{2}\right) \qquad (1)$$

[1]Géosciences Rennes, UMR 6118, Université de Rennes, CNRS, Rennes, France.

where ω is the power average exponent. For the harmonic, geometric and arithmetic means, ω is respectively equal to -1, 0 and 1. For the corresponding layered and random cases, ω thus expresses the dependence of the upscaling rule on the permeability structure. Outside of the three previous cases, expression (1) has not been proven for any other cases. It has however been used to express upscaling results in theoretical as well as in natural permeability fields.

[3]   In this paper, our first objective is to assess the capacity of the power averaging method to express the upscaling law for a wider range of permeability structures. Our second objective is to better understand the influence of permeability structures on upscaling. Our methodology consists in numerically determining the power average exponent ω for various permeability structures. We then analyze the relation between ω and the geometrical characteristics of the structures. After reviewing the basics of power averaging and synthesizing the existing values of ω (section 2), we describe the permeability structures and numerical methods (section 3) used to obtain the values of ω reported in section 4. We finally discuss the relations between ω and the morphological characteristics of the permeability fields (section 5).

2.   Basics on the Use of Power Averaging for Upscaling

2.1.   Theoretical Foundations of Power Averaging

[4]   Power averaging has been first proposed for characterizing the effective permeability of sand-shale formations
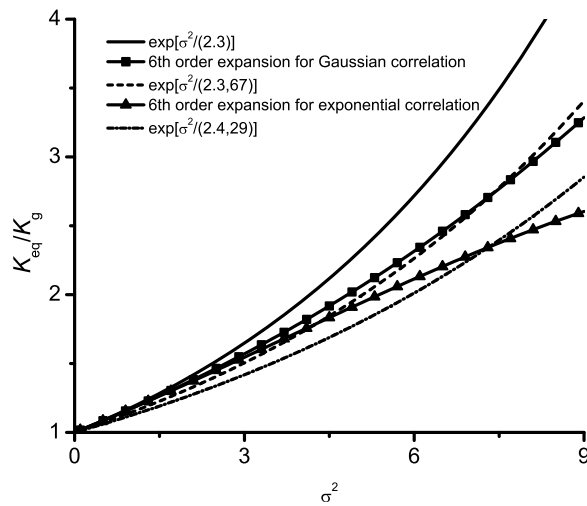
Figure 1. Equivalent permeability for 3D isotropic lognormal permeability fields. Plain lines with symbols indicate the 6th order approximation in σ [*De Wit*, 1995]. Fitting the sixth order expression of *de Wit* [1995] by the exponential expression (1) gives $\omega = 1/3.67$ for the exponential case and $\omega = 1/4.29$ for the Gaussian case. Fits are represented by the dashed and dotted curves.

[*Journel et al.*, 1986]. *Desbarats* [1992a] defined the power averaging formula from the spatial average of the conductivity field over a volume V:

$$K_V = \left(\frac{1}{V} \int_V [K(x)]^\omega dV \right)^{\frac{1}{\omega}} \quad for \ \omega \neq 0 \qquad (2)$$

$$K_V = \exp\left(\frac{1}{V} \int_V \ln(K(x)) dV \right) \quad for \ \omega = 0 \qquad (3)$$

K_V is equal to the arithmetic mean at point scale ($\omega = 1$) and decreases to an asymptotic value for large volumes. The rate of decrease and convergence is a function of the variogram of the permeability field and of the boundary conditions [*Desbarats*, 1992b]. The asymptotic value is however independent of the boundary conditions at least for classical 2D lognormally distributed finitely correlated fields [*Desbarats*, 1992b; *Sánchez-Vila et al.*, 2006]. The maximum value of ω is 1 and corresponds to flow parallel to a layered structure. The minimum value of ω is -1 and corresponds to flow perpendicular to a layered structure. For lognormally distributed permeability fields, (2) and (3) lead to the more compact equation (1).

[5] Apart for the trivial cases $\omega = -1$ and 1, the power averaging method has been rigorously demonstrated only for 2D lognormally distributed permeability fields in which case $\omega = 0$ [*Matheron*, 1967]. As the proof of Matheron is essential for this study and difficult to find in English, we recall it in Appendix A. More generally, upscaling for lognormally distributed and finitely correlated isotropic permeability fields has been conjectured by *Landau and Lifshitz* [1960] to follow the exponential expression (1) whatever the Euclidean dimension E with [*Gelhar and Axness*, 1983; *Paleologos et al.*, 1996]

$$\omega = 1 - \frac{2}{E} \qquad (4)$$

[6] In 1D and 2D, equation (4) is correct with $\omega(1D) = -1$ and $\omega(2D) = 0$. In 3D, The exponential expression (1) is consistent with perturbation expansions in the local correlations to all orders [*Noetinger*, 1994], showing its relevance for negligible correlation lengths. For correlated permeability fields, (4) is consistent with renormalization group results [*Noetinger*, 2000] and with perturbation expansions up to the fourth order in the standard deviation of the permeability logarithm σ [*De Wit*, 1995]. It differs however from the sixth order perturbation expansion in σ [*Abramovich and Indelman*, 1995; *De Wit*, 1995]. The difference is equal to $-0.000467 \ \sigma^6$ for exponential fields and to $-0.0014 \ \sigma^6$ for Gaussian fields. The exponential conjecture given by (1) and (4) is thus different from De Wit's results, but not far from it. In fact, the closest exponential fits to the sixth order expansion formulae give maximum errors of the order of 10% (Figure 1). Finally, a heuristic argument against the power average expression (1) for 3D media as well as for all other types of media is that, for very large σ^2, the flow structure is extremely channeled in 1D highly tortuous channels made up of the largest permeabilities, inducing in turn a decrease of the power average exponent ω with σ^2. For systems at percolation threshold, this argument is consistent with critical path analyses [*Ambegaokar et al.*, 1971].

[7] The exponential expression has also been inferred for anisotropic permeability fields from second-order perturbation expansions in σ both in 2D and 3D [*Dagan*, 1989; *Gelhar and Axness*, 1983]. The power average exponent depends both on the anisotropy rate and on the direction of flow compared to the anisotropy. The 3D exponential expression has been challenged by a fourth order perturbation expansion in σ [*Indelman and Abramovich*, 1994].

[8] To summarize, theoretical foundations for the power average expression remain so far limited to series and parallel models and to 2D lognormally correlated fields. Even though the power average expression may only approximate the upscaling law, it has still been used as a practical way to express permeability upscaling.

2.2. Power Average Exponents for Lognormal Permeability Distributions

[9] The power averaging expression (1) has been used in several studies to present upscaling results. For an unconfined aquifer, 2D Monte Carlo simulations led to power average exponents $\omega = -0.2$ and $\omega = -0.4$ for conditional and unconditional simulations [*Gómez-Hernández and Gorelick*, 1989]. From synthetic slug tests in classical 3D lognormally distributed permeability fields, averaging has been performed by accounting for the convergent flow configuration [*Beckie and Harvey*, 2002]. Permeabilities are weighted inversely proportionally to the square of the distance to the well [*Desbarats*, 1994]. The power average exponent ω grows from -0.19 to 0.345 with the ratio of the characteristic scale of the heterogeneity to the characteristic scale of the averaging volume. For 2D fracture networks having power law fracture length distributions and lognormal fracture transmissivity distributions, ω varies between -1 and 1 and depends on the fracture power law length exponent and on the fracture density [*de Dreuzy et al.*, 2001b]. ω increases with the fracture density and with the frequency of larger fractures.

[10] Two studies have also looked for the geometrical properties controlling the variations of ω. For 2D soil
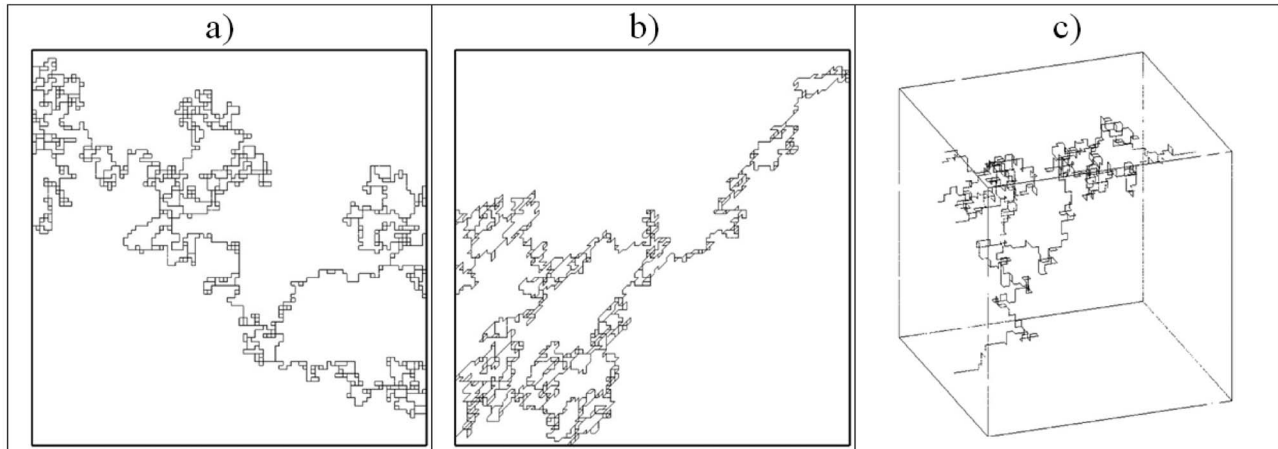
Figure 2. On-lattice (a) 2D square, (b) 2D triangular and (c) 3D cubic backbones (flowing structures) at percolation threshold for a system size normalized by the element length of 100.

structures with lognormal pore size distributions, simulations of unsaturated flow related the power average exponent ω to integrated flow properties of the porous medium through a critical path analysis [*Samouëlian et al.*, 2007]. ω is expressed as a power law function of t_0/m_c where t_0 "is the smallest conductivity which has to be passed on the most efficient path through the structure" and m_c is "the critical mass fraction of conductivities larger than t_0 required finding a continuous path" [*Samouëlian et al.*, 2007, p. 1182] For 2D branching channel networks with a binary distribution of permeabilities, ω ranges between 0 and 0.5 [*Ronayne and Gorelick*, 2006]. It increases with the channel continuity and it is inversely proportional to the fractal dimension and tortuosity. These two studies thus show that ω depends both on global metric and topological properties of the structure.

[11] Finally, the power average exponent ω has been used itself as a characterization means. *Knudby and Carrera* [2005] used it as a channeling index for porous and porous fractured media and *Scheibe and Yabusaki* [1998] used it for predicting transport properties.

3. Structures and Numerical Methods

[12] As our objective, at this point, is to assess the relevance of the power averaging expression (1) for permeability upscaling, we have chosen simple structures and simulation methods.

3.1. Permeability Structures

[13] Permeability structures are on-lattice percolation-like structures (Figure 2). Percolation structures are one of the most classical models for highly heterogeneous porous and fractured media [*Berkowitz and Balberg*, 1993; *Berkowitz and Ewing*, 1998; *Hunt and Ewing*, 2009]. Besides their direct relevance to natural media, they are simple and provide a large diversity of hydraulic behaviors well characterized in the physics literature [*Stauffer and Aharony*, 1992]. Displaying fractal properties at percolation threshold, they behave like effective media above. Their properties are fundamentally determined either by the embedding Euclidean dimension or by their coordination number (maximum number of closest

neighbors by node). We have selected 2D square and triangular networks and 3D cubic network differing by their embedding Euclidean dimension or their coordination number. The square and triangular networks have the same Euclidean dimension 2 but differ by their coordination number equal respectively to 4 and 6. The triangular and cubic networks have the same coordination number 6 but different embedding Euclidean dimensions equal to 2 and 3 respectively.

[14] For a given type of network, all hydraulic properties are controlled by a single order parameter p called the parameter of percolation. For on-lattice structures, p is the proportion of occupied bonds. Networks are connected when p is larger than its value at threshold p_c whatever the embedding system size. The percolation threshold depends on the Euclidean dimension and on the coordination number [*Galam and Mauger*, 1996]. For on-lattice square, triangular and cubic networks, p_c is equal respectively to 0.5, 0.347 and 0.249. The percolation threshold p_c depends both on the coordination number and the embedding Euclidean dimension. All other characteristics are only function of the embedding Euclidean dimension [*Stauffer and Aharony*, 1992]. The fractal dimension of the backbone (flowing structure) is equal to 1.6 in 2D and 1.74 in 3D whatever the coordination number. Other examples are the scaling of the number of red links and of permeability at percolation threshold. Red links are defined as the links that disconnect the network if removed. Their number scales with the system size with a power of 0.75 in 2D and 1.14 in 3D. The equivalent permeability decreases with the system size to the power of −0.98 in 2D and −2.28 in 3D [*Batrouni et al.*, 1996; *Grassberger*, 1999].

[15] Most percolation studies have been focused on structures with identical elements. The importance of each element is solely function of its position within the structure. Some studies have also dealt with networks made up of differing elements. The element specificity is introduced by an additional local permeability distribution. Each element has its own permeability. Upscaling consists, first, in deriving the equivalent permeability of the structure and, second, in comparing it with the local permeability distribution. Former studies have shown that, at percolation threshold, upscaling laws depend both on the network structure and

on the type of the local permeability distribution. For power law distributions of local permeabilities $p(k) \sim k^{-\alpha}$ with $0 < \alpha < 1$, the scaling of the equivalent permeability is modified. The equivalent permeability decreases faster than without permeability distribution [*Feng et al.*, 1987]. The fundamental reason of the additional decrease has been explained using critical path analysis [*Ambegaokar et al.*, 1971; *Hunt*, 2001; *Katz and Thompson*, 1986]. It is induced by the red links having the smallest permeability acting as strong obstacles. For this power law decrease of permeability, the scaling of the equivalent permeability is modified but remains universal, i.e., only dependent on the Euclidean dimension. For a log-uniform permeability distribution, *Charlaix et al.* [1987] computed bounds for the equivalent permeability. These bounds have different pre-factors but the same permeability scaling as without permeability distribution. Their main conclusion is that the log-uniform permeability distribution induces a significant increase of the size of the representative elementary volume (REV).

[16] To summarize, percolation-like structures have both common and specific properties. Their permeability and red-link number scalings and their fractal dimension at threshold are universal in the sense that they only depend on the embedding Euclidean dimension. However, they differ by their local characteristics like the coordination number. One of the objectives of this paper is to find whether the power average exponent ω depends only on the Euclidean dimension like the universal percolation-theory exponents or also on the coordination number like the percolation threshold.

3.2. Local Permeability Distribution and Flow Simulation

[17] We studied upscaling numerically by simulating flows on the previous structures with a local permeability distribution. The local permeability distribution is imposed on top of the structure by drawing a permeability for each link of the network. We used uncorrelated lognormal and log-uniform distributions as local permeability distribution. Their parameters are their lognormal mean and variance μ and σ^2. For the lognormal distribution, the equivalent permeability being linearly proportional to the exponential of μ, we keep σ^2 as the sole parameter for the local permeability distribution. Drawing random number in the lognormal distribution relies on the sampling of the centered normal distribution by the Box-Muller method. The result is then transformed to get the targeted lognormal distribution.

[18] The flow model is based on mass conservation and on Darcy's law within the elements leading to $\nabla((Kg/\nu)\nabla h) = 0$, where h stands for the hydraulic head, ν for the kinematic viscosity, g for the gravity constant and K for the element permeability. Simple permeameter-like boundary conditions are applied on the system borders. Two opposite borders have fixed head and all other borders are impervious. Discretization of the flow equation is performed by applying Darcy's laws between the nodes and mass conservation at intersections [*de Dreuzy et al.*, 2001a]. Discretization leads to a linear system of dimension proportional to the number of nodes. The linear system is solved either with multifrontal or conjugate gradient preconditioned by algebraic multigrid methods implemented respectively in the UMFPACK and HYPRE software [*Davis and Duff*, 1999; *Falgout et al.*, 2005]. Multifrontal methods are direct methods orders of magnitude faster

than iterative methods for this kind of network problems [*de Dreuzy and Erhel*, 2003]. We use them for most not too large matrices, i.e., of dimension lower than 10^7 for 2D and 10^6 for 3D. For larger matrices, we use an algebraic multigrid based method requiring less memory. The algebraic multigrid method had to be used as the preconditioner of a conjugate gradient in order to get systematically a solution [*Erhel et al.*, 2009]. Solving linear systems of dimensions 10^6 in 2D and 5.10^5 in 3D takes respectively around 4 and 5 min on an Intel Xeon 3GHz 16 Go workstation. With these methods, the limiting factor of the simulation does not come from solving the linear system but from the generation of the networks. For each set of parameters, we perform 500 Monte Carlo simulations. The total number of simulations necessary to get the results presented in sections 4 and 5 is of the order of 10^5.

3.3. Determination of ω

[19] The equivalent permeability K is computed from the total input flow to the system Q_{in}, the head differences between the system inlet and outlet Δh, the system size L, and the Euclidean dimension E according to

$$K = \frac{\nu}{g} \frac{Q_{in}}{\Delta h \cdot L^{E-2}} \qquad (5)$$

What we call the system size denoted by L is fundamentally the system size normalized by the elementary link size. For a given simulation, the equivalent permeability depends on the system structure, on the local permeability distribution and on the realization specificities. The system structure is parameterized by the network type denoted "*type*," the parameter of percolation p and the system size L. The local permeability distribution is parameterized by the logarithmic standard deviation σ. The realization specificities are the seeds and the nature of the random number generator that we identify under the index i, i standing for the ith simulation. We thus write the equivalent permeability as $K(\sigma, type, p, L, i)$.

[20] This study is focused on the influence of the network structure on the upscaling of the local permeability distribution. For complex structures, the equivalent permeability without permeability distribution is no longer K_{G} as expressed by the power average expression (1). We denote it $K(\sigma = 0, type, p, L, i)$ and generalize expression (1) in
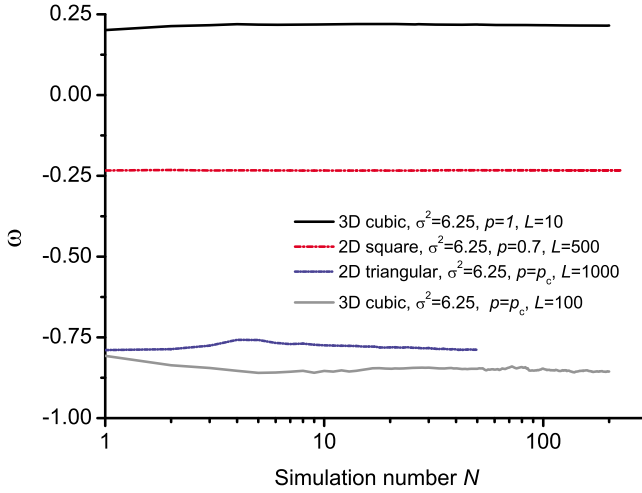
$$K(\sigma, type, p, L, i) = K(\sigma = 0, type, p, L, i) \cdot f(\sigma, type, p, L, i) \quad (6)$$

where f is a function equal to 1 for $\sigma = 0$. For the power average expression (1) f takes the following exponential form:

$$f(\sigma, type, p, L, i) = \exp\left[\frac{\omega(\sigma, type, p, L, i) \cdot \sigma^2}{2}\right]. \qquad (7)$$

[21] For more general permeability distributions, expression (2) leads to

$$f(\sigma, type, p, L, i) = \left(\frac{K_G(\mu, \sigma)}{K_H(\mu, \sigma)}\right)^{\omega(\sigma, type, p, L, i)} = \left(\frac{K_A(\mu, \sigma)}{K_G(\mu, \sigma)}\right)^{\omega(\sigma, type, p, L, i)}$$

$$(8)$$

Figure 3. Convergence of ω with the simulation number N.

[22] From equations (6) and (7), we derive the power average exponent ω on a realization basis for lognormal local permeability distributions:

$$\omega(\sigma, type, p, L, i) = \frac{2}{\sigma^2} \cdot \ln\left(\frac{K(\sigma, type, p, L, i)}{K(\sigma = 0, type, p, L, i)}\right). \quad (9)$$

[23] For different permeability distributions, equations (6) and (8) give

$$\omega(\sigma, type, p, L, i) = \ln\left(\frac{K(\sigma, type, p, L, i)}{K(\sigma = 0, type, p, L, i)}\right) \Big/ \ln\left(\frac{K_A(\mu, \sigma)}{K_G(\mu, \sigma)}\right). \quad (10)$$

[24] Determining ω for the realization i from (9) or (10) requires thus to perform two simulations on the same structure with and without the local permeability distribution. We have checked that the logarithmic variance σ^2 of the lognormal permeability distribution does not depend on the realization i. For example, for networks made up of 10^4 links, the variability of σ^2 is lower than 1%.

[25] Finally, we perform Monte Carlo simulations to obtain the mean and standard deviation of the power averaging exponents $\omega(\sigma, type, p, L, N)$ and $\sigma[\omega(\sigma, type, p, L, N)]$, where N is the number of Monte Carlo simulations:

$$\omega(\sigma, type, p, L, N) = \langle\omega(\sigma, type, p, L, i)\rangle_{1 \leq i \leq N} \quad (11)$$

$$\sigma^2[\omega(\sigma, type, p, L, N)] = \langle[\omega(\sigma, type, p, L, i) \\ - \omega(\sigma, type, p, L, N)]^2\rangle_{1 \leq i \leq N} \quad (12)$$

[26] We dropped the angle brackets in the notation of ω of the left-hand term side of equation (11) to keep it simple; and in the rest of the article, the notation ω always refers to its mean value. We thus adopt a realization-based approach rather than an ensemble approach by first determining ω on a realization basis and then averaging the calculated values
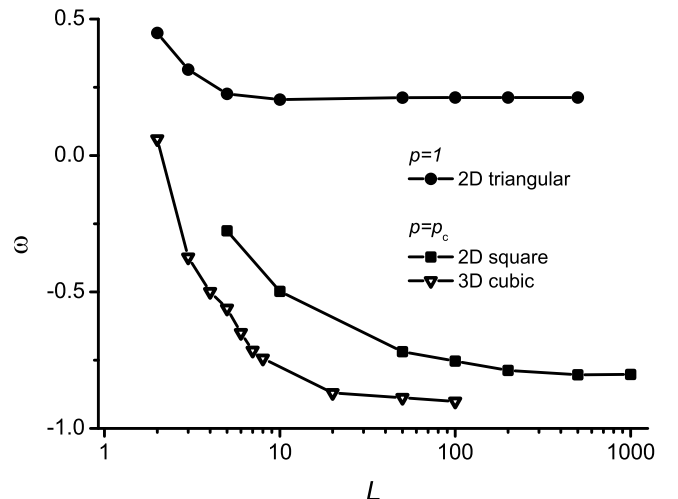
of ω in order to filter out as much as possible the realization effects.
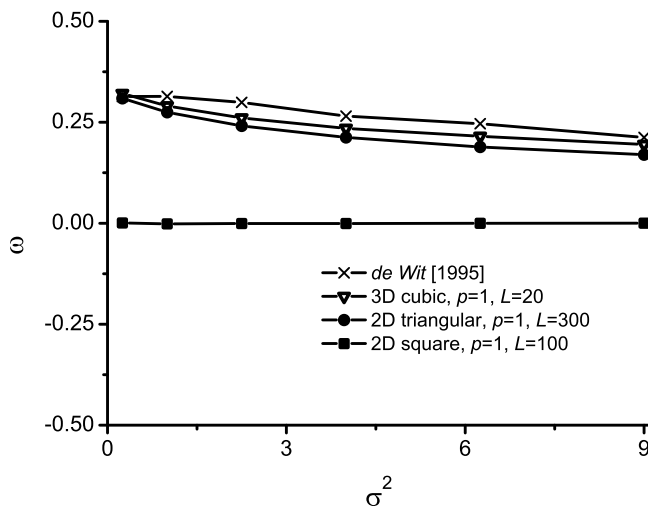
4. Results

[27] We recall that the objectives of this study are, first, to assess the relevance of the power average expression (6) for upscaling and, second, to determine the relations between ω and the network structure. In the terms of the notation of the previous section, the first objective is to analyze the dependency of $\omega(\sigma, type, p, L, N)$ with σ. The less it depends on σ, the more relevant is the power averaging expression. The second objective is to study the dependence of $\omega(\sigma, type, p, L, N)$ on the structure type (*type*) and on the density factor p. We are thus interested in the dependence of ω on σ, *type* and p and neither on the system size L nor on the number of Monte Carlo simulations N. That is why we first show that $\omega(\sigma, type, p, L, N)$ converges with L and N to $\omega(\sigma, type, p)$. Second, we assess that $\omega(\sigma, type, p)$ in fact does not depend on σ. Third, we study the dependence of $\omega(type, p)$ on *type* and p.

4.1. Convergence of ω With the Number of Simulations N and the System Size L

[28] At large system sizes L and for a large σ^2 value of 6.25, the convergence of ω is reached for 10 to 200 simulations depending on the network type (Figure 3). As a general rule convergence is faster for dense networks than for networks at the percolation threshold and for smaller σ^2. The number of simulations has been systematically chosen in order that the variability of ω around its mean value for the second half of the simulations is smaller than 0.005. For all explored cases, ω also converges with the system size L within the explored range of scales (Figure 4). The rate of convergence is very fast for networks above percolation threshold whereas it is much slower for networks at percolation threshold. Simulations were performed till the largest computationally possible size equal to 100 for 3D networks and 1000 for 2D networks. Computational limits are due to generation times for all cases. The difference of ω between

Figure 4. Convergence of ω with the system size L with $\sigma^2 = 4$.

DE DREUZY ET AL.: UPSCALING PERMEABILITY IN COMPLEX MEDIA

Figure 5. Dependence of ω on σ^2 for dense networks. Crosses stand for the value of ω derived from the perturbation results of *de Wit* [1995] for the exponential correlation function (Figure 1).

Figure 6. Dependence of ω on σ^2 for networks at the percolation threshold.

its values at the maximal size L_{max} and at half of it is limited to 0.015 in the worst case. The largest system sizes are thus large enough to assimilate the limiting value $\omega(\sigma, type, p)$ to $\omega(\sigma, type, p, L_{max})$ with a maximum precision of 0.02 corresponding to the addition of the potential errors coming from the finite number of simulations and finite scale. This value of 0.02 is 1% of the full range of ω values [−1,1].

4.2. Assessment of the Relevance of the Power Average Expression for Upscaling
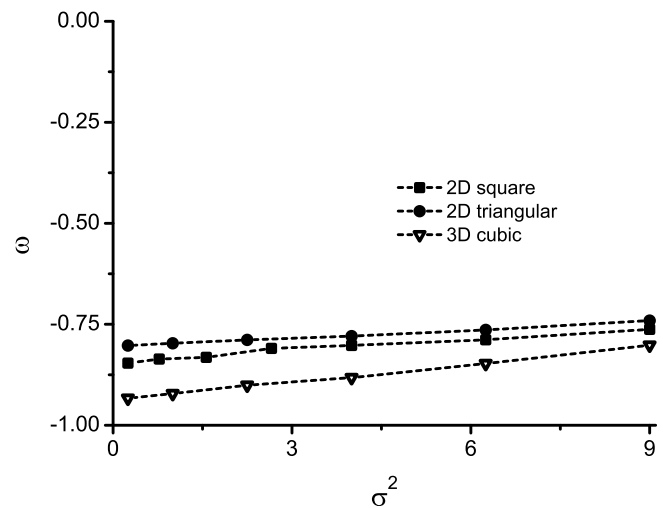
[29] The fundamental interest of power averaging (1) is to provide a simple formula separating the effect of the structure in ω and of the local permeability variability in K_g and σ^2. Its relevance directly depends on the invariance of ω with σ^2. For dense 2D square networks, it is strictly the case (Figure 5, solid squares). Variations of ω around 0 are limited to 10^{-3} (Table 1). Table 1 and Figure 5 also show that ω is independent of σ^2 only for the 2D square case and not for the 2D triangular case. In fact the demonstration of Matheron recalled in Appendix A requires implicitly the existence of the geometrical invariance by a 90° rotation of the network structure. It is the case only for the dense 2D square networks and not for the other cases.

[30] For the dense 2D triangular and 3D cubic networks, ω varies slightly with σ^2 without systematic tendencies (Figure 5). The standard deviation of ω ($\sigma(\omega)$) varies between 0.04 and 0.05 and its amplitude of variation ($\omega_{max} - \omega_{min}$) ranges between 0.12 and 0.14 (Table 1). These values are

significantly larger than the precision of determination of 0.02. They should be compared to the amplitude of the full possible range of ω values equal to 2 as ω varies within [−1,1]. ω thus varies between 6% and 7% of the full possible range of values. These variations being nonnegligible, the power average expression is not strictly valid. However, it gives already an estimate at a few percent of the upscaled permeability. Variations of ω with σ^2 are smaller at percolation threshold (Figure 6 and Table 2). The standard deviation of ω ($\sigma(\omega)$) varies between 0.01 and 0.03 and its amplitude of variation ($\omega_{max} - \omega_{min}$) ranges between 0.03 and 0.09. ω thus varies between 1.5% and 4.5% of the full possible range of values.

[31] Although ω is not strictly independent of σ^2, its variations are still limited. This goes against the heuristic argument that ω should systematically significantly decrease with σ^2 because of more extreme flow channeling. It is indeed not the case as ω may either increase or decrease with σ^2 (Figures 5 and 6). The possible flaw in the previous argument could be that the increased channeling comes also with a refined selection of the higher permeability values. Both effects leading to opposite consequences, they compensate and lead only to a slight increase or a slight decrease of ω.

4.3. Dependence of ω on the Network Type and on the Percolation Parameter p

[32] For dense networks, ω is equal to 0 for 2D square networks consistently with Matheron's demonstration (see Appendix A). For 3D cubic networks, the mean value of ω is equal to 0.25 and is significantly different from 1/3.

Table 1. Minimum, Maximum, Average, Standard Deviation and Variation Range of ω as a Function of σ^2 for Dense Networks With a Lognormal Local Permeability Distribution[a]

Network Type	ω_{min}	ω_{max}	$\langle\omega\rangle$	$\sigma(\omega)$	$\omega_{max} - \omega_{min}$
2D square	-1×10^{-3}	7×10^{-4}	-4×10^{-4}	8×10^{-4}	0.002
2D triangular	0.17	0.31	0.23	0.05	0.14
3D cubic	0.20	0.32	0.25	0.04	0.12

[a]For on-lattice networks, $p = 1$. For off-lattice networks, $p = 2p_c$.

Table 2. Minimum, Maximum, Average, Standard Deviation and Variation Range of ω as a Function of σ^2 for Networks at Threshold With a Lognormal Local Permeability Distribution

Network Type	ω_{min}	ω_{max}	$\langle\omega\rangle$	$\sigma(\omega)$	$\omega_{max} - \omega_{min}$
2D square	−0.85	−0.76	−0.81	0.03	0.09
2D triangular	−0.80	−0.77	−0.78	0.01	0.03
3D cubic	−0.93	−0.85	−0.90	0.03	0.08
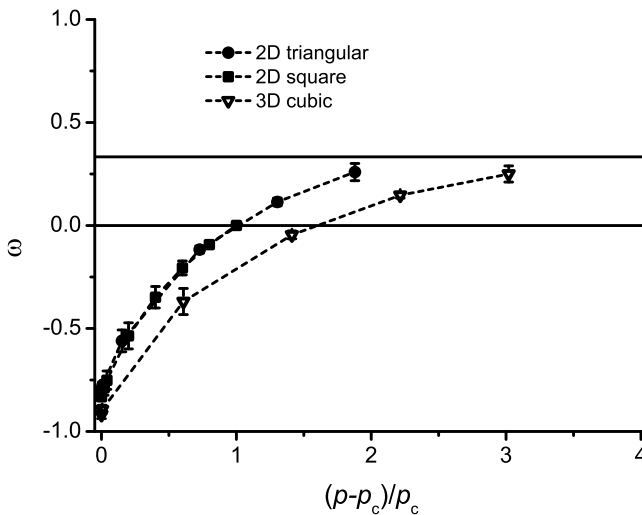
Figure 7. Dependence of ω on density represented as the rate above the percolation threshold.

We recall that the precision of ω is of the order of 0.02. However, the maximal value of ω is equal to 0.32 for $\sigma^2 = 0.25$. Agreement with equation (4) improves for values of σ^2 close to 0 and deteriorates for σ^2 larger than 1 (Figure 4). We also compared the 3D cubic values of ω to the prediction of *De Wit* [1995] for the exponential correlation case represented by triangles in Figure 1 and equivalently by crosses in Figure 5. These numerical results are much closer to De Wit's approximation than to equation (4). We finally note that, for the dense case, the 2D triangular case has ω values close to those of the 3D cubic case. As the 2D triangular and 3D cubic cases have the same coordination number of 6, it suggests that the coordination number may be a key controlling parameter at least for dense networks.

[33] We have also computed ω for several smaller values of p. Because of the limited variability of ω with σ^2, we present the average of ω with respect to σ^2 as a function of the normalized distance to the percolation threshold $((p - p_c)/p_c)$ (Figure 7). As expected, ω increases monotonously with p as adding more links increases the number of possible paths. Compared to its increase, its variability represented by the error bars is much smaller confirming that power averaging provides for a good estimate of upscaling. Values of ω for the square and triangular cases increase exactly along the same tendency showing in turn the relevance of the normalized distance to the percolation threshold $((p - p_c)/p_c)$ as a basic controlling parameter for 2D on-lattice networks. The 3D on lattice case remains close to the 2D on lattice case. The maximum difference between ω values is of the order of 0.15. We note however that the values of ω for 3D networks remain systematically lower than the values of ω for 2D lattices.

[34] After having commented the increase, we focus now only on the range of variations of ω. At percolation threshold, values of ω are minimal and range between -0.78 and -0.9 (Table 1). These values never reach -1 as would predict critical path analysis [*Katz and Thompson*, 1986]. In fact, for critical path analysis, the upscaled permeability is exclusively controlled by the red links forming a system in series controlled by its smallest permeabilities. This argument has been successively applied to power law distributions of permeabilities [*Feng et al.*, 1987] but is not strictly valid here for the lognormal permeability distributions, which extreme are less pronounced. On the other end, for dense networks, ω becomes close to 1/3. Considering all cases, ω can take at least all values in a large interval between -0.9 and 0.3.

5. Discussion

[35] Permeability upscaling is basically controlled by metric and topological properties [*Havlin and Ben-Avraham*, 1987]. Typical metric properties are the tortuosity, the fractal dimension of the backbone at threshold or the distribution of distances between two points within the backbone. The power average exponent would for example strongly depend on existing correlations between the local permeability and this inter-point distance [*de Dreuzy et al.*, 2001b]. Typical topological properties are the coordination number and the topological diffusion exponent in percolation theory [*Havlin and Ben-Avraham*, 1987]. The question here is to find whether ω is controlled by metric features, by topological features or by both together. The previous results already show that ω does not behave like the universal exponents of percolation theory as for square and triangular 2D networks at threshold have significantly different ω values. We have also seen that the control by the density term p is only partial (Figure 7). The dependence of ω with this term is consistent only for the 2D triangular and square networks and not for the 3D cubic networks.

5.1. Dependence of ω on the Coordination Number

[36] The results of section 4 indicate that a controlling parameter may be the coordination number. In fact the 3D cubic and 2D triangular networks have the same coordination number and very close values of ω in the dense case (Table 1). The classically used coordination number in percolation theory q is the maximum number of neighbors per point [*Galam and Mauger*, 1996]. Here we introduce a new "effective coordination number" c defined as the average number of neighbor per point within the backbone ($2 \leq c \leq q$). The power average exponent ω is expected to increase monotonously with c. In fact more neighbors per point enhances the possibilities to avoid small permeabilities and in turn lets the macroscopic permeability increase. In other simpler words, increasing the effective coordination number c makes the network structure more "parallel-like."

[37] The dependence of ω on c is shown in Figure 8 for the on-lattice networks as well as for Cayley trees. Cayley trees are pure hierarchical loop-less tree structures for which permeability upscaling can be simply computed by performing alternatively harmonic and arithmetic averages [*Stauffer and Aharony*, 1992]. Figure 8 shows that ω values for on-lattice and Cayley trees follow globally the same increasing trend with the effective coordination number.

[38] Two regimes can be identified. For $c \geq 3$, i.e., above percolation threshold, all on-lattice values of ω follow closely the same trend with an accuracy less than 0.05, showing the relevance of the effective coordination number. The average tendency given by the solid line of Figure 8 has not been obtained by fitting the data but as the exponential function respecting the three following endmost models: 1) for $c = 2$, links are in series and $\omega = -1$; 2) $c = 4$ corresponds
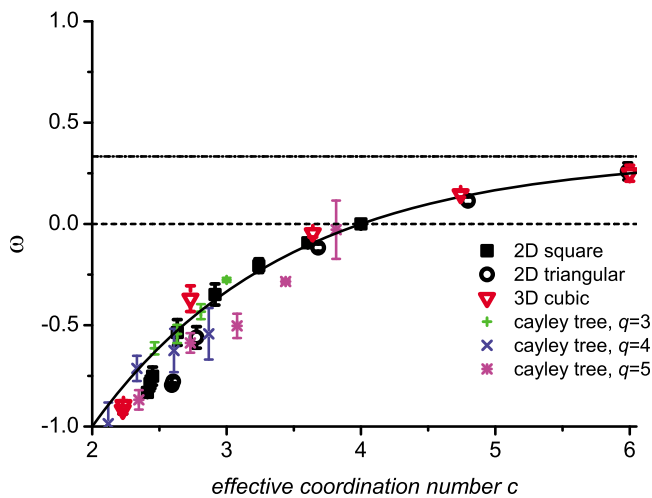
Figure 8. Dependence of ω on the effective coordination number (average number of neighbors per intersection point in the backbone).

among other possibilities to the 2D square case for which $\omega = 0$; 3) the limit of the exponential is set to $\omega = 1/3$ equal to the 3D prediction given by equation (4). It leads to the following approximate dependence ω_{app} on the effective coordination number c:

$$\omega_{app}(c) = \frac{1}{3} - \frac{4}{3} \cdot 2 - \frac{4}{c-2} \quad (13)$$

ω_{app} is precise at 0.05 for $c \geq 3$, and at 0.1 for 2D square and 3D cubic on-lattice networks for $c < 3$ and at 0.2 for 2D triangular on-lattice networks. In this latter regime ($2 \leq c < 3$), the effective coordination number itself does not explain all the variations of ω. On one hand, the normalized distance to the percolation threshold $(p - p_c)/p_c$ remains much more consistent for the square and triangular 2D on-lattice networks than the effective coordination number (Figure 7). On the other hand, 3D cubic and 2D triangular values of ω are better explained by coordination number. Around percolation threshold, upscaling does not depend on a single parameter but on a combination of topological and metric properties like the effective coordination number and the normalized distance to the percolation threshold.

[39] To get insight into the role of connectivity concealed in the effective coordination number, we compare the results obtained on the on-lattice networks to those obtained on Cayley trees. The interest of Cayley trees is that they are solely characterized by topological characteristics, which are the coordination number q (maximum possible number of neighbor per point) and the effective coordination number c (average number of neighbor per point). Figure 8 shows that ω increases with c and decreases with q (crosses and stars). The main tendency is the increase with c while the decrease with q is of secondary importance. We also note that the variability of ω with σ^2 represented on Figure 8 by the error bars is on average 2.5 times larger than for the other network cases. The variability of ω with σ^2 decreases from Cayley trees to on-lattice networks. The relevance of power averaging for upscaling improves thus when increasing the disorder of the structure. For $2 \leq c < 3$, values of ω

for the on-lattice networks and for the Cayley trees fall into the same range. Precisely at threshold ($2 \leq c < 2.5$), we have already seen that topological properties cannot by themselves explain all the variations of ω. However, for $2.5 \leq c < 3$, ω values for the 2D on-lattice square and triangular cases are close to those of the Cayley trees for $q = 3$ and $q = 5$ respectively. These values are lower by one unit than the coordination number $q = 4$ and $q = 6$ of the square and triangular networks. ω values for the 3D cubic on-lattice networks are slightly further away from those of the Cayley trees.

[40] Like the previous studies on unsaturated soils [*Samouëlian et al.*, 2007] and on channel networks [*Ronayne and Gorelick*, 2006], we relate the power average exponent to simpler morphological characteristics. But there is a difference in the nature of the controlling characteristics. The previous studies relate ω to global properties like the critical conductivity and mass fraction or to fractal dimension and tortuosity. Here we do not relate ω to a global but to a local morphological property (the effective coordination number).

5.2. Robustness of ω With the Local Permeability Distribution

[41] As shown by the previous results, the power average exponent ω is controlled much more by the structure of the medium parameterized by the type of network "type" and by the density p than by the variance of the lognormal local permeability distribution. But does it depend also on the shape of the local permeability distribution at fixed lognormal mean and variance? We handle this question by comparing the ω values obtained with the previous lognormal distribution to those obtained with log-uniform distributions for the 2D square and 3D cubic networks. We use the same methodology as for the lognormal distribution and use equation (8) instead of equation (7) to compute ω. ω converges both with the number of realizations and with the
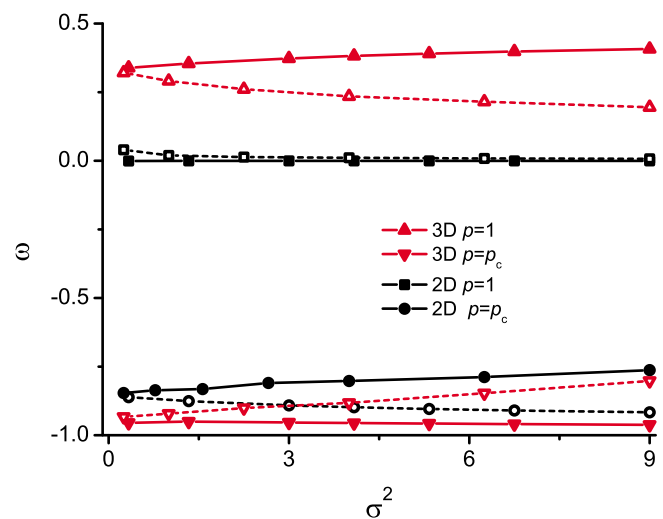
Figure 9. Dependence of ω on the local permeability distribution shape for 2D square and 3D cubic networks. Solid symbols and lines stand for the log-uniform distribution while open symbols and dashed lines stand for the lognormal distribution.

Table 3. Minimum, Maximum, Average, Standard Deviation and Variation Range of ω as a Function of σ^2 With a Log-Uniform Local Permeability Distribution

Network Type	ω_{min}	ω_{max}	$\langle \omega \rangle$	$\sigma(\omega)$	$\omega_{max} - \omega_{min}$
2D square, $p = p_c$	-0.92	-0.86	-0.89	0.03	0.06
2D square, $p = 1$	-7×10^{-4}	-4×10^{-4}	-5×10^{-4}	2×10^{-4}	0.0003
3D cubic, $p = p_c$	-0.96	-0.95	-0.95	0.01	0.01
3D cubic, $p = 1$	0.34	0.41	0.38	0.03	0.07

system size with very similar conditions as for the lognormal case.

[42] Besides being comparable to the lognormal distribution, the additional interest of the log-uniform distribution is that the logarithm of the distribution is symmetrical and thus respects the assumptions of Matheron's demonstration (see Appendix A). In fact, we found that, for square dense on-lattice networks ($p = 1$), the mean and standard deviation are both smaller than 10^{-3} (Table 3). On average the variability of ω as measured by its standard deviation $\sigma(\omega)$ is two times smaller for the log-uniform distribution showing that the power averaging method is even more appropriate for the log-uniform than for the lognormal distribution. Apart from the 2D square on-lattice dense case, differences induced by the shape of the distribution are nonnegligible. They amount to -0.08 and -0.05 for the 2D and 3D cases at threshold and to $+0.13$ for the 3D dense case ($p = 1$) (Figure 9). The variability due to the permeability distribution is thus much larger than the variability induced by σ^2. We finally note that differences increase with larger σ^2.

[43] We have not however studied the dependence of ω on the choice of the boundary conditions. All simulations have been performed with permeameter-like boundary conditions. Values of ω for large scales might be the same like in the dense square on-lattice case for which the equivalent permeability is the geometric average both for parallel and convergent flows [*Sánchez-Vila et al.*, 2006]. This should be confirmed in a future study for all other configurations. It would also be important to assess in the future the influence of other structure characteristics like anisotropy or large-range correlations.

6. Conclusion

[44] We have assessed the relevance of the power averaging expressions (2) and (3) for permeability upscaling with extensive numerical simulations on a variety of 2D and 3D, dense and sparse on-lattice structures. We have determined the power average exponent ω according to expressions (9) and (10) for respectively lognormal and log-uniform local permeability distributions. ω has been determined on a realization basis, i.e., by deriving first its value for a given realization by comparing the equivalent permeabilities both with and without local permeability distributions and second by averaging its values over several realizations. Convergence of ω was reached with the number of simulations and with the system size within the range of scales explored. The maximum precision of the determination of ω is equal to

0.02, a value that corresponds to 1% of the full possible interval of variation of ω $[-1,1]$. The results presented come from around 10^5 simulations.

[45] The relevance of power averaging has been assessed by analyzing the dependence of ω as a function of the variance of the local permeability distribution σ^2 on the broad interval of values $[0,9]$. Power averaging is strictly valid only for the 2D dense square case for which ω is equal to 0 with a precision of 0.01 both for the lognormal and log-uniform permeability distributions. This is consistent with the theoretical proof of *Matheron* [1967] recalled in Appendix A. For the 3D dense cubic case, ω is close to 0.33 only for small values of σ^2 and is much closer to *De Wit*'s [1995] sixth order expansion in σ than to the conjecture of *Landau and Lifshitz* [1960]. For all other cases, ω is significantly not constant as its variability according to σ^2 is larger than the precision of its determination 0.02. Despite this non-negligible variability, power averaging gives a first approximation of upscaling at a few percents of precision. In fact the difference between extreme values of ω for $\sigma^2 \in [0,9]$ is equal to 0.08 for sparse networks and 0.14 for dense networks representing respectively 4% and 7% of the full possible range of ω values. The relevance of power averaging seems to improve with more disorder as the maximal imprecision significantly decreases from Cayley trees to on-lattice networks. We have also showed that power averaging is slightly more appropriate for log-uniform rather than for lognormal distributions, and that the power average exponent ω depends on the shape of the local permeability distribution at equal variances.

[46] Globally, we found that ω takes values in the broad interval $[-0.9,0.5]$. Most of the variations of ω can be explained by the effective coordination number. The effective coordination number is the average number of neighbors per point in the flowing structure (backbone), not to confound with the coordination number defined as the maximum number of possible neighbors per point. ω increases with the effective coordination number as the possibilities to avoid smaller permeability values itself increases. The control by the effective coordination number is confirmed by the similarities of ω values with those of Cayley trees, structures solely determined by coordination. The control is especially strong above percolation threshold while at percolation threshold the broader dispersion of values reflects the higher complexity of the network structure. The general perspective of this work is to better understand with a wider set of permeability patterns the relation between morphology and permeability upscaling.

Appendix A: Matheron's Demonstration for Upscaling Permeability in 2D Isotropic Heterogeneous Fields

[47] We recall here the demonstration of *Matheron* [1967] showing that the equivalent permeability is the geometric average of the spatial permeability distribution for 2D isotropic permeability fields k for which $\frac{k}{E(k)}$ and $\frac{k^{-1}}{E(k^{-1})}$ follow the same distribution.

[48] We first define the upscaling operator F from the micro-scale permeability distribution $p(k)$ to the macro-scale equivalent permeability $F(k)$. At the micro scale, flows

are modeled by Darcy's law expression and the conservation of mass:

$$q = -k\nabla h$$
$$\nabla \cdot q = 0 \tag{A1}$$

where q, k and h are the microscopic flow. At the macro scale, the equivalent permeability is $F(k)$ derived from (A1) by

$$F(k) = -\frac{E(q_i)}{E(\partial_i h)} \tag{A2}$$

where i is a generic index for the direction x or y and $\partial_i h$ is the partial derivative of h in the direction i. In 2D isotropic media, flow lines and constant head lines are perpendicular. A rotation of $\pi/2$ exchanges a gradient field into a conservative field (divergence free field) and conversely. The gradient field ∇h is transformed into a conservative field $f\left(-\frac{\partial h}{\partial y}, \frac{\partial h}{\partial x}\right)$ of divergence equal to 0: $\nabla f = 0$. The conservative field q is transformed into a field $p(-q_y, q_x)$ deriving from a gradient g such as $p = \nabla g$. From (A1), f and g are linked by $f = -\frac{1}{k}\nabla g$. The transformed fields follow a system analogous to (A1):

$$f = -\frac{1}{k}\nabla g$$
$$\nabla f = 0 \tag{A3}$$

[49] As this system as the same structure as the system (A1), the upscaling operator is also F leading to

$$F\left(\frac{1}{k}\right) = -\frac{\mathrm{E}(f_i)}{\mathrm{E}(\partial_i g)}$$

[50] Because of the equality between $\frac{\mathrm{E}(f_i)}{\mathrm{E}(\partial_i g)}$ and $\left(\frac{E(q_i)}{E(\partial_i h)}\right)^{-1}$:

$$F(k^{-1}) = \frac{1}{F(k)}. \tag{A4}$$

[51] For a microscopic permeability distribution k for which $\frac{k}{E(k)}$ and $\frac{k^{-1}}{E(k^{-1})}$ have the same distribution, the upscaling operator has the same value for both of these distributions:

$$F\left(\frac{k}{E(k)}\right) = F\left(\frac{k^{-1}}{E(k^{-1})}\right). \tag{A5}$$

[52] Because of the linearity of the flow equation, the upscaling operator is also linear transforming equation (A5) in

$$F(k)/F(k^{-1}) = E(k)[E(k^{-1})]^{-1}. \tag{A6}$$

[53] From (A5) and (A6), we deduce that

$$F(k) = \sqrt{E(k)[E(k^{-1})]^{-1}}. \tag{A7}$$

[54] The upscaled permeability is thus the geometric mean of the arithmetic and harmonic means. Equivalently, the upscaled permeability is the geometric average of the local permeabilities. For a lognormal distribution of permeability of logarithmic mean and variance μ and σ^2, $F(k) = \exp(\mu)$. We underline that the upscaling result of (A7) is not only valid for the 2D isotropic lognormal permeability distribution but more generally for all 2D isotropic permeability distributions for which $\frac{k}{E(k)}$ and $\frac{k^{-1}}{E(k^{-1})}$ have the same distribution including the log-uniform distribution.

References

Abramovich, B., and P. Indelman (1995), Effective permittivity of lognormal isotropic random-media, *J. Phys. A. Math. Gen.*, *28*(3), 693–700.

Ambegaokar, V., B. I. Halperin, and J. S. Langer (1971), Hopping conductivity in disordered systems, *Phys. Rev. B Solid State*, *4*(8), 2612–2620, doi:10.1103/PhysRevB.4.2612.

Batrouni, G. G., A. Hansen, and B. Larson (1996), Current distribution in the three-dimensional random resistor network at the percolation threshold, *Phys. Rev. E*, *53*, 2292–2297, doi:10.1103/PhysRevE.53.2292.

Beckie, R., and C. F. Harvey (2002), What does a slug test measure: An investigation of instrument response and the effects of heterogeneity, *Water Resour. Res.*, *38*(12), 1290, doi:10.1029/2001WR001072.

Berkowitz, B., and I. Balberg (1993), Percolation theory and its application to groundwater hydrology, *Water Resour. Res.*, *29*(4), 775–794, doi:10.1029/92WR02707.

Berkowitz, B., and R. P. Ewing (1998), Percolation theory and network modeling applications in soil physics, *Surv. Geophys.*, *19*(1), 23–72, doi:10.1023/A:1006590500229.

Cardwell, W. T., and R. L. Parsons (1945), Averaging permeability of heterogeneous oil sands, *Trans. Am. Inst. Min. Metall. Pet. Eng.*, *160*, 34–42.

Charlaix, E., E. Guyon, and S. Roux (1987), Permeability of a random array of fractures of widely varying apertures, *Transp. Porous Media*, *2*, 31–43, doi:10.1007/BF00208535.

Cushman, J. H. (1986), On measurement, scale and scaling, *Water Resour. Res.*, *22*(2), 129–134, doi:10.1029/WR022i002p00129.

Cushman, J. H., L. S. Bennethum, and B. X. Hu (2002), A primer on upscaling tools for porous media, *Adv. Water Resour.*, *25*(8–12), 1043–1067.

Dagan, G. (1989), *Flow and Transport in Porous Formations*, 465 pp., Springer, Berlin.

Davis, T. A., and I. S. Duff (1999), A combined unifrontal multifrontal method for unsymmetric sparse matrices, *Trans. Math. Software*, *25*(1), 1–20, doi:10.1145/305658.287640.

de Dreuzy, J. R., and J. Erhel (2003), Efficient algorithms for the determination of the connected fracture network and the solution of the steady-state flow equation in fracture networks, *Comput. Geosci.*, *29*, 107–111, doi:10.1016/S0098-3004(02)00081-X.

de Dreuzy, J. R., P. Davy, and O. Bour (2001a), Hydraulic properties of two-dimensional random fracture networks following a power law length distribution: 1. Effective connectivity, *Water Resour. Res.*, *37*(8), 2065–2078.

de Dreuzy, J. R., P. Davy, and O. Bour (2001b), Hydraulic properties of two-dimensional random fracture networks following a power law length distribution: 2. Permeability of networks based on log-normal distribution of apertures, *Water Resour. Res.*, *37*(8), 2079–2095, doi:10.1029/2001WR900010.

Desbarats, A. J. (1992a), Spatial averaging of hydraulic conductivity in three-dimensional heterogeneous porous media, *Math. Geol.*, *24*(3), 249–267, doi:10.1007/BF00893749.

Desbarats, A. J. (1992b), Spatial averaging of transmissivity in heterogeneous fields with flow toward a well, *Water Resour. Res.*, *28*(3), 757–767, doi:10.1029/91WR03099.

Desbarats, A. J. (1994), Spatial averaging of hydraulic conductivity under radial flow conditions, *Math. Geol.*, *26*(1), 1–21, doi:10.1007/BF02065873.

De Wit, A. (1995), Correlation structure dependence of the effective permeability of heterogeneous porous-media, *Phys. Fluids*, *7*(11), 2553–2562, doi:10.1063/1.868705.

Erhel, J., J. R. de Dreuzy, A. Beaudoin, E. Bresciani, and D. Tromeur-Dervout (2009), A parallel scientific software for heterogeneous hydrogeology, *Parallel Comput. Fluid Dyn.*, *2007*, 39–48.

Falgout, R. D., J. E. Jones, and U. M. Yang (2005), Pursuing scalability for HYPRE's conceptual interfaces, *Trans. Math. Software*, *31*(3), 236–350, doi:10.1145/1089014.1089018.

Feng, S., B. I. Halperin, and P. N. Sen (1987), Transport properties of continuum systems near the percolation threshold, *Phys. Rev. B*, *35*(1), 197–214, doi:10.1103/PhysRevB.35.197.

Galam, S., and A. Mauger (1996), Universal formulas for percolation thresholds, *Phys. Rev. E*, *53*(3), 2177–2181, doi:10.1103/PhysRevE.53.2177.

Gelhar, L. W., and C. L. Axness (1983), Three-dimensional stochastic analysis of macrodispersion in aquifers, *Water Resour. Res.*, *19*(1), 161–180, doi:10.1029/WR019i001p00161.

Gómez-Hernández, J. J., and S. M. Gorelick (1989), Effective groundwater model parameter values: Influence of spatial variability of hydraulic conductivity, leakance, and recharge, *Water Resour. Res.*, *25*(3), 405–419, doi:10.1029/WR025i003p00405.

Grassberger, P. (1999), Conductivity exponent and backbone dimension in 2-D percolation, *Physica A*, *262*(3–4), 251–263, doi:10.1016/S0378-4371(98)00435-X.

Havlin, S., and D. Ben-Avraham (1987), Diffusion in disordered media, *Adv. Phys.*, *36*(6), 695–798, doi:10.1080/00018738700101072.

Hunt, A. G. (2001), Applications of percolation theory to porous media with distributed local conductances, *Adv. Water Resour.*, *24*(3–4), 279–307, doi:10.1016/S0309-1708(00)00058-0.

Hunt, A., and R. Ewing (2009), Porous media primer for physicists, in *Percolation Theory for Flow in Porous Media*, pp. 57–96, Springer, Berlin.

Indelman, P., and B. Abramovich (1994), A higher-order approximation to effective conductivity in media of anisotropic random structure, *Water Resour. Res.*, *30*(6), 1857–1864, doi:10.1029/94WR00077.

Journel, A. G., C. V. Deutsch, and A. J. Desbarats (1986), Power averaging for block effective permeability, paper presented at 56th California Regional Meeting, Soc. of Pet. Eng., Oakland, Calif.

Katz, A. J., and A. H. Thompson (1986), Quantitative prediction of permeability in porous rock, *Phys. Rev. B*, *34*, 8179–8181, doi:10.1103/PhysRevB.34.8179.

Knudby, C., and J. Carrera (2005), On the relationship between indicators of geostatistical, flow and transport connectivity, *Adv. Water Resour.*, *28*(4), 405–421, doi:10.1016/j.advwatres.2004.09.001.

Landau, L. D., and E. M. Lifshitz (1960), *Electrodynamics of Continuous Media*, Pergamon, New York.

Matheron, G. (1967), *Eléments Pour une Théorie des Milieux Poreux*, Masson, Paris.

Neuman, S. P., and V. Di Federico (2003), Multifaceted nature of hydrogeologic scaling and its interpretation, *Rev. Geophys.*, *41*(3), 1014, doi:10.1029/2003RG000130.

Noetinger, B. (1994), The effective permeability of a heterogeneous porous medium, *Transp. Porous Media*, *15*(2), 99–127, doi:10.1007/BF00625512.

Noetinger, B. (2000), Computing the effective permeability of log-normal permeability fields using renormalization methods, *C. R. Acad. Sci. Ser. IIA Sci. Terre Planetes*, *331*(5), 353–357.

Paleologos, E. K., S. P. Neuman, and D. Tartakovsky (1996), Effective hydraulic conductivity of bounded, strongly heterogeneous porous media, *Water Resour. Res.*, *32*(5), 1333–1341, doi:10.1029/95WR02712.

Renard, P., and G. d. Marsily (1997), Calculating equivalent permeability: A review, *Adv. Water Resour.*, *20*(5–6), 253–278, doi:10.1016/S0309-1708(96)00050-4.

Ronayne, M. J., and S. M. Gorelick (2006), Effective permeability of porous media containing branching channel networks, *Phys. Rev. E*, *73*(2), 026305, doi:10.1103/PhysRevE.73.026305.

Samouëlian, A., H. J. Vogel, and O. Ippisch (2007), Upscaling hydraulic conductivity based on the topology of the sub-scale structure, *Adv. Water Resour.*, *30*(5), 1179–1189, doi:10.1016/j.advwatres.2006.10.011.

Sánchez-Vila, X., J. Carrera, and J. P. Girardi (1996), Scale effects in transmissivity, *J. Hydrol.*, *183*(1–2), 1–22, doi:10.1016/S0022-1694(96)80031-X.

Sánchez-Vila, X., A. Guadagnini, and J. Carrera (2006), Representative hydraulic conductivities in saturated groundwater flow, *Rev. Geophys.*, *44*, RG3002, doi:10.1029/2005RG000169.

Scheibe, T., and S. Yabusaki (1998), Scaling of flow and transport behavior in heterogeneous groundwater systems, *Adv. Water Resour.*, *22*(3), 223–238, doi:10.1016/S0309-1708(98)00014-1.

Stauffer, D., and A. Aharony (1992), *Introduction to Percolation Theory*, 2nd ed., Taylor and Francis, Bristol, U. K.

Wen, X.-H., and J. J. Gómez-Hernández (1996), Upscaling hydraulic conductivities in heterogeneous media: An overview, *J. Hydrol.*, *183*, ix–xxxii, doi:10.1016/S0022-1694(96)80030-8.

P. Davy, P. de Boiry, J.-R. de Dreuzy, and G. Pichot, Géosciences Rennes, UMR 6118, Université de Rennes, CNRS, Campus de Beaulieu, F-35042 Rennes CEDEX, France. (jean-raynald.de-dreuzy@univ-rennes1.fr)